Oral Presentation

The 7th TSME International Conference on Mechanical Engineering
13-16 December 2016

TSME ICOME 2016
Mechanical Engineering Innovation for Green Society

DRC0010

A Modelling Approach for Soft Pectoral Fins of a Carangiform Fish Robot

Anh Pham Van[1], Tien Nguyen Tan[1] and Quan Tuong Vo[1,*]

[1] Faculty of Mechanical Engineering, Ho Chi Minh City University of Technology, 268 Ly Thuong Kiet, Ward 14, Dist. 10, Ho Chi Minh City, 84, Vietnam
[*]vtquan@hcmut.edu.vn, +840933327078

Abstract

The pectoral fins play an important role in supporting and stabilizing the locomotion of fishes in nature. This concept is also considered for the biomimetic fish robots. This paper proposes the approach of modelling for the soft pectoral fins of a biomimetic Carangiform fish robot. Firstly, a model of fundamental frequencies and mode shapes of non-uniform fins are built which is based on Rayleigh's method. Secondly, the dynamical model of the pectoral fins in fluid is derived by the combination of the Lagrange method, the Assume Mode Method (AMM) and the Morison's formula. The hydrodynamic forces impact along the pectoral fins surface are considered as the drag force and the inertial force corresponding with the influences of added mass and damping of fluid. Then, the simulations are implemented to verify the feasibility of the proposed mathematical model in following cases: free vibration mode, the change of the stimulating input torques to the soft fin deformation and the generated thrust in forced vibration mode. Finally, several comparisons and analysis are carried out to show effectiveness of the proposed modelling.

Keywords: Soft pectoral fin, Carangiform, Fish robot, AMM, Morison, Lagrange.

1. Introduction

Natural fishes underwent a long time of evolution, the natural selection retained nearly every diversify of remarkable adaptation for locomotion, especially the types of self-propulsion in locomotion. Comparing to traditional propellers or jets, the like-fish moving mechanisms exhibit a superiority excellent maneuverability, low energy consumption and good adaptation to the surrounding environment. Therefore, the approaches of fish inspired robot research have witnessed a growing applications in emergence, exploration, environmental research and military area [1]. Most of fishes generate thrust by undulating their bodies into a propulsive wave that can extend to the caudal fin, a type of swimming classified under body and/or caudal fin (BCF) locomotion [2]. The greatly achieved thrust and movement acceleration are this regime characteristics. The median and/or paired fin (MPF) propulsion use the undulation or oscillation of fins as pectoral fin pelvic, anal, and dorsal to generate the thrust. Greater maneuverability, higher stability and better propulsive efficiency but slower motion speed are than BCF locomotion.

Many researchers focused on developing fish-inspired robots using multi-link mechanism undulating the body and tail part to generate thrust and swimming movements [3-5]. This selection aims to mimic the physical structures as the BCF fish backbone. The robot has good maneuverability. However, the control cost is high by redundant structures. Some other studies use the rigid fin forms [6]. Smart actuators such as SMAs, IPMCs or LZT owing ability to perform flexible and complex movements also used in biomimetic underwater robots [7-9], In [9], a flexible and lightweight pectoral fin embedded SMA material is studied. Koi Carp fin motion is captured from experiment results and used to control artificial fin rays. This is able to perform the complexity motions. However, this is kinematic motion of fin rays.

Flexible fin are much interesting in biomimetic robotic area. With much advantages of high thrust performance, silent motion. In the research [10], a kinematic analyst of compliant caudal fin is conducted to identify the maximum thrust velocity. Although this is based on the kinematic model and experimental research but it can be used as a guideline to design fins of bio-inspired robot. A two links robot mathematical model using the rigid body and a flexible caudal fins is considered in [10, 11]. The Euler - Bernoulli theory and Morison's equation are used to establish the relation between effect of encompassing fluid and tip-fin displacement. However, the fin input signals supplied by servomotor is a function of angle. The Euler - Bernoulli approach for flexible tail is also used in the research [12]. This considered the resistive force acting on the body of fin as a term analogous of viscous damping. Nevertheless, this consider the tail fins as non-uniform in the one dimension. A different approach to the flexible fins is also mentioned in [13]. The interaction system of fluid and a flexible plate are considered on base of the finite element method. However, this approach is computerized time consuming and complex to design controllers.

The pectoral fins in BCF mode have an important role in maneuverable thrust and they are also vital for balancing, braking and movement supporting, etc. The thrust mechanism generated by the pectoral fins is quite widespread among fish species. Although, it's difficult to observe and analyze due to the variability and complexity of movements such as flapping, rotations and undulations. Several researches of the pectoral are conducted in recent time such as in [6, 9, 14]. According to [15], there are two main oscillatory

movement types for the pectoral fins: drag-based methods and lift-based methods. In [6], the drag based mode is used to design a pair of the pectoral fins which work as paddles. Although, the velocity obtaining is low and the fins producing thrust is rigid fins. In other research about the pectoral fin, a model of beam liked pectoral fin is mentioned in [16], though this approach is applied to uniform pectoral fins.

A type of the pectoral fins using MPF mode is also developed in robot form as Manta or Cow-nose Ray fish by high swimming efficient and good stabilization. In [17], a novel bionic fish, Cow-nose Ray robot is designed to obtain optimal swimming velocity. However, the proposed design is kinematic model.

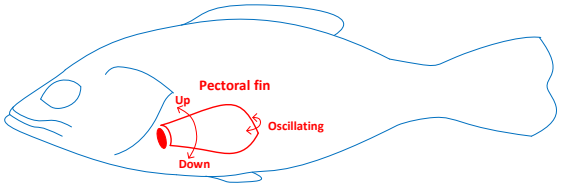

Fig.1 An operation type of pectoral fin on the life fish

Almost the BCF fish species mainly use the both of tail fin and pectoral fins to travel in water. Inspired by the pectoral fin of life fish (Fig.1), a model of robotic fish driven is developed. The robot must have ability of extremely smooth moving and good pitch, yaw angle stabilization to support for camera device inside. In order to satisfy these criterion, a pair of soft pectoral fins are added to enhance the maneuverability stabilization of robot.

In this paper, we propose a mathematical model of a symmetrical non-uniform flexible pectoral fins actuated by 2 DOFs (degree of freedoms) intermediate joints in fluid. Based on Lagrange method, AMM approach and Morison's equation, the hydrodynamic motion of fin in fluid is expanded explicitly. With the achieved model, a type of fin profile is chosen to simulate and validate the fin deformation responses and produced thrust force.

The paper is organized as follows. First, a brief review of the modeling of robotic fish fin in fluids is reviewed. Second, configuration of the mechanism, fundamental frequency and mode shape of flexible fin are presented. Then, the hydrodynamic modeling using combination of AMM and Lagrange equation is discussed. In this mathematical description, the external forces acting on along of a slender fin proposed are the Morison force. In section 4, the simulation results are conducted to evaluate the effectiveness of the proposed method. Finally, conclusions are summarized in section 5.

2. Structure of the mechanism and the solutions of eigenvalue problem

To research on the operational mechanism of the Carangiform fish robot using a pair of soft pectoral fins elaborately, the interaction of generated moment. Therefore, the configuration of a pectoral fin is separated from main body of fish robot is considered. The mechanism of a pectoral fin includes two intermediate joints and a non-uniform flexible fin. The joints are actuated by the torque motors.

The motion structure of the flexible pectoral fin is shown on the Fig. 2.

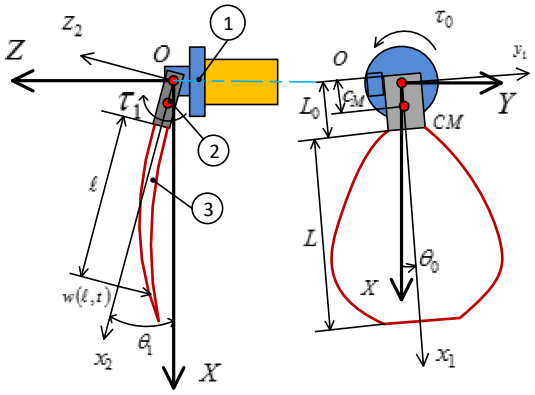

Fig. 2 Schematic representation of pectoral fin coordinate

The pectoral fin parts are regarded in the earth fixed coordinate. The link 1, actuated by the torque t_0, can turn around a fixed axis in the earth frame. The link 2, actuated by the torque t_1 can twist an axes perpendicular to the link 1 axes. The coordinates are defined as: $OXYZ$, $o_1x_1y_1z_1$, $o_2x_2y_2z_2$ express the earth fixed frame, the link 1 fixed frame, the link 2 (the fin hinge and the flexible fin frame) respectively. The 2-DOF driving structure allows that fish robot can generate many complex motion with high maneuverability.

According to AMM, deformation of flexible pectoral fin can be described by below expression:

$$w(l) = \sum_{i=1}^{N} s_i(t)\,\varphi_i(l) \qquad (1)$$

Where, $s_i(t)$ is the i[th] modal coordinate and presented in the next section, $\varphi_i(l)$ is the i[th] mode shape function.

The mode shape function and natural frequencies can be found by solving the eigenvalue problem accurately. This is applied to uniform beam commonly. However, it is difficult to derive from non-uniform fin. According to [18], the profile of tail fin is approximated by exponential function. So, it can be simpler to determined eigenvalue problem. In this paper, we use the Rayleigh-Ritz method [19] for the determination of the fundamental frequencies and mode shapes of pectoral fin.

To employ the method, the harmonic excitation function of ω and magnitude $\varphi(x)$ is assumed to apply to system. The quantity Φ is defined as:

$$\Phi = T_{\max} - V_{\max} \qquad (2)$$

Where, the maximum kinetic energy:

$$T_{\max} = \frac{w^2}{2}\int_0^L \rho A(x)\varphi^2(x)\,dx \qquad (3)$$

And the maximum potential energy:

$$V_{\max} = \frac{1}{2}\int_0^L EI(x)\left(\frac{d^2\varphi}{dx^2}\right)^2 dx \quad (4)$$

The Rayleigh-Ritz procedure is used to determine the natural frequency and corresponding mode shapes. By substituting Eq. (3) and Eq. (4) into Eq. (2). The expression is rewritten as:

$$F = \frac{\omega^2}{2}\int_0^L \rho A(x)\varphi^2(x)dx - \frac{1}{2}\int_0^L EI(x)\left(\frac{d^2\varphi(x)}{dx^2}\right)^2 dx \quad (5)$$

We assume a solution of the form:

$$\varphi(x) = \sum_{n=1}^{N} c_n f_n(x) \quad (6)$$

Where $f_n(x)$ is the trial function, c_n is the undetermined coefficient. Rewrite Eq. (5), we have:

$$F = \frac{1}{2}\sum_{p=1}^{N}\sum_{l=1}^{N} c_l c_p G_{pl} \quad (7)$$

Where:

$$G_{pl} = \omega^2\int_0^L \rho A(x) f_l(x) f_p(x)dx - \int_0^L EI(x) f_l''(x) f_p''(x)dx \quad (8)$$
$$= \omega^2 I_{1,pn} - I_{2,pn}$$

Where: $I_{1,pn} = \int_0^L \rho A(x) f_l(x) f_p(x)dx$ (9)

And $I_{2,pn} = \int_0^L EI(x) f_l''(x) f_p''(x)dx$ (10)

The prime denotes the derivative with respect to x. The Rayleigh-Ritz method states that a necessary condition for a stationary value of ω is attained when:

$$\frac{\partial\Phi}{\partial c_n} = 0, \quad n = 1,2,...N. \quad (11)$$

Substituting Eq. (7) into Eq. (11) and performing the indicated operation, the following system of N equations in terms of N unknown constants c_l is obtained:

$$\frac{\partial}{\partial c_n}\left(\sum_{p=1}^{N}\sum_{l=1}^{N} c_l c_p G_{pl}\right) = 2\sum_{l=1}^{N} c_l G_{nl} = 0 \quad (12)$$

Transforming Eq. (12) over several steps, we derive:

$$\omega^2\sum_{l=1}^{N} c_l I_{1,nl} - \sum_{l=1}^{N} c_l I_{2,nl} = 0 \quad (13)$$

In matrix form, we can rewritten as:

$$[I_2]\{c\} - \omega^2[I_1]\{c\} = 0 \quad (14)$$

The Eq. (14) is a standard eigenvalue equation from ω and the corresponding mode shape can be determined, once $I_{1,nl}$, and $I_{2,nl}$ have been determined. By arranging the eigenvalues in ascending order and normalizing $\varphi(x)$ to a unitary fin tip deformation, that satisfies condition: $\varphi(L) = 1$, the mode shapes of the pectoral fins can be established.

3. Hydrodynamic modeling

In order to derive the mathematical model motion of the pectoral fin in fluid, some assumptions are proposed as below: the fin vibrates along its fundamental mode shapes; the deformation of flexible fin only includes the bending displacement along the longitudinal direction, neglecting the deformation of the fin in other directions. Due to the great influence of the first mode shapes on the dynamic deformation of fin, an approximate solution for the bending displacement and propulsion mechanism are proposed. We also assume that the effects of the gravity force on the pectoral fin and the buoyancy force generated by surrounding fluid are ignored.

In this paper, the Lagrange method is used to establish the mathematical model of the thrust force produced by mechanism of a pectoral fin in fluid environment.

$$\frac{d}{dt}\left(\frac{\partial L}{\partial \dot{q}_i}\right) - \frac{\partial L}{\partial q_i} = Q_i \quad (15)$$

Where, $L = T - V$ is the Lagrange function, Q_i is external generalized forces. In this research, we ignore the damping of rotational joints. Therefore, the external generalized forces include the fluid forces: impact on the surface of the soft pectoral fin.

The kinetic energy of the link 1 is given below:

$$T_0 = \frac{1}{2} I_0 \dot{q}_0^2 \quad (16)$$

Where I_0 is the inertial moment of the link 1.

The kinetic energy of the link 2 is expressed in the form:

$$T_1 = \frac{1}{2} m_1 {}^0v_1^T {}^0v_1 + \frac{1}{2} {}^0w_1^T \left({}^1I_1\right) {}^0w_1 \quad (17)$$

Where m_1 is the mass of the link 2. The term ${}^0v_1$ is the global translational velocity of the central mass of the link 2 expressed in the base frame $OXYZ$. We note that the left superscript and right subscript of letters indicate the corresponding coordinates in the equations. ${}^0w_1$ is the angular velocity which maps from the earth fixed frame $OXYZ$ to frame $o_1x_1y_1z_1$ and expressed as:

$${}^0w_1 = {}^0R_1 {}^1w_1 \quad (18)$$

Where ${}^0R_1$ is the rotational transformation matrix from fixed frame $OXYZ$ to the frame $o_1x_1y_1z_1$, ${}^1w_1$ is the corresponding angular velocity of the link 2 in frame $o_1x_1y_1z_1$

$${}^1w_1 = \begin{bmatrix} 0 & \dot{q}_1 & 0 \end{bmatrix}^T \quad (19)$$

$${}^0I_1 = {}^0R_1 {}^1I_1 {}^0R_1^T \quad (20)$$

The expression of ${}^0v_1$ is determined as:

$${}^0v_1 = J \begin{bmatrix} \dot{q}_0 \\ \dot{q}_1 \end{bmatrix} \quad (21)$$

Where: J is Jacobian matrix determined by the following expression:

$$J = \begin{bmatrix} c_M \sin q_0 \cos q_1 & -c_M \cos q_0 \sin q_1 \\ c_M \cos q_0 \cos q_1 & -c_M \sin q_0 \sin q_1 \\ 0 & c_M \cos q_1 \end{bmatrix} \quad (22)$$

Where c_M is the distance from central mass of the link 2 to the origin O.

The term ${}^1I_1$ is called the moment of inertia tensor of the link 2 expressed in the frame $o_1x_1y_1z_1$.

$${}^0I_1 = \begin{bmatrix} I_{xx}\cos^2 q_0 + I_{yy}\sin^2 q_0 & \frac{1}{2}(I_{xx} - I_{yy})\sin 2q_0 & 0 \\ \frac{1}{2}(I_{xx} - I_{yy})\sin 2q_0 & I_{xx}\sin^2 q_0 + I_{yy}\cos^2 q_0 & 0 \\ 0 & 0 & I_{zz} \end{bmatrix} (23)$$

Where I_{xx}, I_{yy}, I_{zz} are the link 2's symmetry inertial tensor.

Substituting Eqs. (19), (21), (23) into Eq. (17), the final expression of the link 2 kinetic energy:

$$T_1 = \frac{1}{2}mc_M^2\left(\dot{q}_0^2\cos^2 q_1 + \dot{q}_1^2\right) + \frac{1}{2}\dot{q}_1^2\left(I_{xx}\sin^2 q_0 + I_{yy}\cos^2 q_0\right) \quad (24)$$

The kinetic energy of flexible fin part (link 3)

$$T_2 = \frac{1}{2}\int_0^L r_F A(x)\left\|{}^0\dot{r}_2\right\|^2 dl \quad (25)$$

Where ${}^0r_2 = {}^0R_2\,{}^2r_2$ and ${}^0R_2$ is the rotational transformation matrix.

The coordinate of a point of the fin on the symmetry plane $o_1x_1z_1$ can be expressed in the $OXYZ$ as:

$${}^0r_2 = \begin{bmatrix} \cos q_1 \cos q_0 & -\sin q_0 & \sin q_1 \cos q_0 \\ \cos q_1 \sin q_0 & \cos q_0 & \sin q_1 \sin q_0 \\ -\sin q_1 & 0 & \cos q_1 \end{bmatrix} \begin{bmatrix} L_0 + l \\ 0 \\ w(l,t) \end{bmatrix} (26)$$

Differentiating the both side of Eq. (26) and substituting into Eq. (25), we derive the kinetic energy of the flexible fin:

$$T_2 = \frac{1}{2}\int_0^L r_F A(l)\left(\dot{q}_0\left((L_0+l)\cos q_1 - w\sin q_1\right)^2 dl + \frac{1}{2}\int_0^L r_F A(l)\left(\dot{w}^2 + 2\dot{w}(L_0+l)\dot{q}_1 + \dot{q}_1^2\left((L_0+l)^2 + w^2\right)\right)dl, \quad (27)$$

Because we only regard to the bending deformation of the flexible fin part, the strain energy can be calculated by:

$$V_2 = \frac{1}{2}E\int_0^L I(l)\left(\frac{\partial^2 w}{\partial l^2}\right)^2 dl \quad (28)$$

Where: E is the elastic modulus of fin material, I is the second moment of fin area.

By combining Eqs. (16), (24), (17-18), we can obtain the expression of Lagrange function:

$$L = T_0 + T_1 + T_2 - V_3 \quad (29)$$

To consider the effect of the external force acting on the whole of fin surface, we use the Morison's force model. Let's denote the normal vector and tangential vector of fin hinge part by $\vec{n}_n$, $\vec{n}_t$ respectively. These vectors are illustrated in the Fig. 3. A similar approach arises in [11].

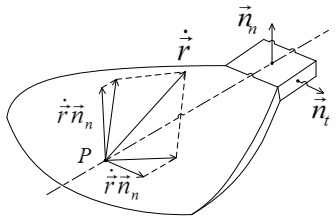

Fig. 3 Representation of the point's velocity on the of the pectoral fin symmetry axes.

We can write the below expressions:

$$\vec{n}_n = \left[\vec{i}_x.\sin q_1 \cos q_0; \vec{i}_y.\sin q_1 \sin q_0; \vec{i}_z.\cos q_1\right] \quad (30)$$

$$\vec{n}_t = \left[\vec{i}_x.\sin q_0; \vec{i}_y.\cos q_0; \vec{i}_z.0\right] \quad (31)$$

Where $\vec{i}_x$, $\vec{i}_x$, $\vec{i}_x$ are unit vectors. By projecting the velocity vector and acceleration vector of one point in flexible fin onto the normal vector $\vec{n}_n$, we can achieve the components of the velocity and acceleration which are perpendicular to the hinge of the flexible fin: $v_n = {}^0\dot{\vec{r}}_2.\vec{n}_n$, $\dot{v}_n = {}^0\ddot{\vec{r}}_2.\vec{n}_n$. Similarly, we can write the components of velocity and acceleration in the tangential direction: $v_t = {}^0\dot{\vec{r}}_2.\vec{n}_t$, $\dot{v}_t = {}^0\ddot{\vec{r}}_2.\vec{n}_t$.

We assume that the Morison's force per unit length acting on the whole of fin surface can be split into two parts. One is perpendicular to the widest plane of hinge plate (see Fig. 3) and another is parallel to the rotational axes of hinge.

$$df_t(1,t) = -\left(r_h p\left(C_{M0} - 1\right)h^2\dot{v}_t + C_{D0}r_h h v_t|v_t|\right)d1, \quad (32)$$

$$df_n(1,t) = -\left(r_h p\left(C_{M1} - 1\right)b^2\dot{v}_n + C_{M1}r_h b v_n|v_n|\right)d1, \quad (33)$$

Where: C_{M0}, C_{M1}, C_{D0}, C_{D1} are the coefficients taking into account the effect of added mass and fluid damping. These coefficients depend on the geometry of fins and Reynolds number of surrounding fluid. r_h is the density of fluid.

Where h, b are a half of thickness and a half of wideness of the pectoral fin respectively.

The external moment impacting on the link 1 is given by the below expression:

$$Q_0(t) = t_0 + Q_{0M}(t) + Q_{0D}(t) \quad (34)$$

Where:

$$Q_{0M}(t) = -\int_0^L \pi\rho_h\left(C_{M0} - 1\right)h^2\dot{v}_t\left(w\sin\theta_1 + \left(L_0 + \ell\right)\cos\theta_1\right)d\ell \quad (35)$$

$$Q_{0D}(t) = -\int_0^L \pi\rho_h C_{D0} h v_t |v_t| \left(w\sin\theta_1 + (L_0+\ell)\cos\theta_1\right) d\ell \quad (36)$$

Similarly, the external moment acting on the link 2 is expressed as:

$$Q_1(t) = t_1 + Q_{1M}(t) + Q_{1D}(t) \quad (37)$$

Where:

$$Q_{1M}(t) = -\int_0^L \pi\rho_h (C_{1M}-1) b^2 \dot{v}_n (L_0+\ell) d\ell \quad (38)$$

$$Q_{1D}(t) = -\int_0^L \pi\rho_h C_{1D} b v_n |v_n| (L_0+\ell) d\ell \quad (39)$$

Based on the virtual work principle, the virtual work of the generalized force acting on surface of fin and causing the generalized displacement to flexible fin can be expressed as:

$$dW(t) = \int_0^L f_n(1,t)\, dw(1,t)\, d1 = \int_0^L f_n(1,t) \sum_{k=1}^{n} j_k(1)\, ds_k(t)\, d1 = \sum_{k=1}^{n} Q_{k+1}(t)\, ds_k(t) \quad (40)$$

Where: $Q_{k+1}(t) = \int_0^L f_n(1,t)\, j_k(1)\, d1$ (41)

The general forces corresponding to the general modes of fin can be divided into two part as:

$$Q_{k+1}(t) = Q_{(k+1)M}(t) + Q_{(k+1)D}(t) \quad (42)$$

Where: $k = 1, N$, N is the used mode number of the pectoral fin

By substituting Eq. (33) into (41) we can obtain the inertial and drag components in Eq. (42) as:

$$Q_{(k+1)M}(t) = -\int_0^L \pi\rho_h (C_{1M}-1) b^2 \dot{v}_n \varphi_k d\ell \quad (43)$$

$$Q_{(k+1)D}(t) = -\int_0^L \pi\rho_h C_{1D} b v_n |v_n| \varphi_k d\ell \quad (44)$$

By combining the Eqs. (29), (34), (37) and (42) into Eq. (15), the motion equation of the system can be derived in the matrix form:

$$M(q)\ddot{q}(t) + D(q,\dot{q})\dot{q} + K(q)q + T_d = T \quad (45)$$

Where: $M(q) = [m_{i,j}]$ is the inertial matrix. $D(q,\dot{q}) = [d_{i,j}]$ is the Coriolis and Centripetal term. $K(q) = [g_{i,j}]$ is the stiffness term. And, $T_d = [T_{d,i}]$ is the external force induced surrounding fluid, EMBED Equation.3 $i, j = 0, N+1$, N is the used mode number. $T = [t_0 \quad t_1 \quad 0 \quad \ldots \quad 0]^T$ is the external torque vector. By solving the Eq. (45) and combining $j(1)$ in the section 2, we can be obtained the deformation with respect to the coordinate 1 and time t.

The thrust force generated by oscillating of the flexible fin part in direction of the pectoral symmetry axis is calculated by the following expression [20]:

$$F_{thrust}(t) = \frac{1}{2} C_T r_h A_f \ddot{Z}(t) \quad (46)$$

Where: C_d is the thrust coefficient, A_f is the area of pectoral fin. $Z(t) = (L_0 + L)\sin q_1 - w(L,t)\cos q_1$ is the displacement of tip fin of pectoral fin projecting onto the direction of axes Z .

4. Simulation results

To illustrate the proposed mathematical model of the pectoral fin, some numerical simulations are implemented. The profile of the pectoral fin mimicked the shape of real fish fin is shown in Fig. 4. The corresponding parameters h, b are a half of thickness and a half of wideness of the pectoral fin used in the preview section.

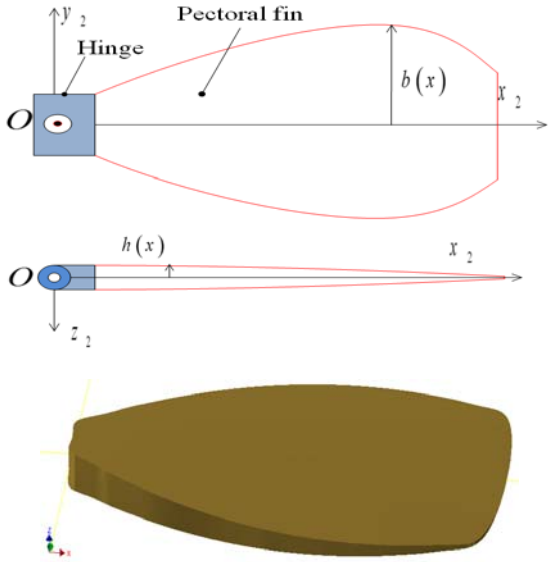

Fig. 4 The profile of proposed pectoral fin

In order to retrieve the profile of the pectoral fin of real fish, a technique using image processing is implemented. This also used in a research about the pectoral fin of Koi Carp fish [14]. The equation of pectoral approximate fin profile is determined by the following equation:

$$\begin{cases} b_1(x) = -6.75x^2 + 0.945x + 0.0075 \\ h_1(x) = -0.0275 + 0.003 \end{cases} \quad (47)$$

The parameters are proposed in the Table. 1

DRC0010

Table. 1

Parameter	Value	Parameter	Value
E	$27.10^6 \left[N/m^2\right]$	r_h	$1200 \left[kg/m^3\right]$
C_{0D}	0.295	L	$0.1\,[m]$
C_{0M}	1.46	L_0	$0.01\,[m]$
C_{1D}	1.28	I_{xx}	$23.10^{-9} \left[kgm^2\right]$
C_{1M}	1.46	I_{yy}	$53.10^{-9} \left[kgm^2\right]$
r_F	$1000 \left[kg/m^3\right]$	I_{zz}	$46.10^{-9} \left[kgm^2\right]$

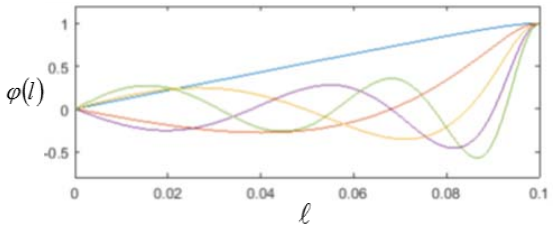

Fig. 5 The five first mode shapes of the flexible pectoral fin part.

Table. 2 Five first natural frequencies of the flexible fin part

$w_1\,[rad/s]$	w_2	w_3	w_4	w_5
9.14	283.14	705.61	1335.37	2179.62

Some fundamental frequencies and mode shapes are shown in the Table. 2 and Fig. 5. We see that the natural frequencies of flexible fin part have significant difference. Some first frequencies affect deeply to the frequency responses of fins. The simulation with free vibration mode is conducted to consider the contribution of the difference mode to general response.

A. Free vibration mode

To show the free motion in fluid of the pectoral fin, we choose the nonzero initial values of the modal coordinate, in detail: $s_1 = s_2 = s_3 = 10^{-4}$ and the simulation time is 0.5 second.

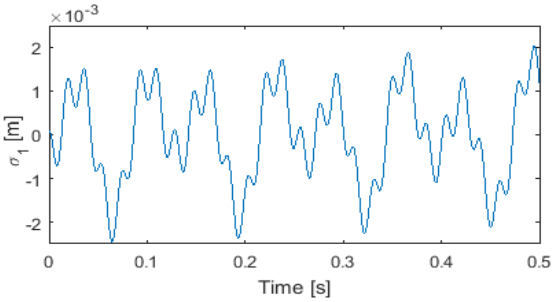

Fig. 6 Performance of the modal coordinate σ_1

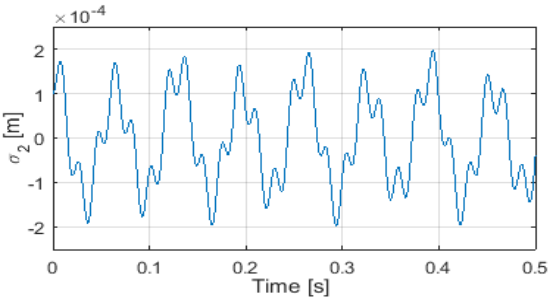

Fig. 7 Performance of the modal coordinate σ_2

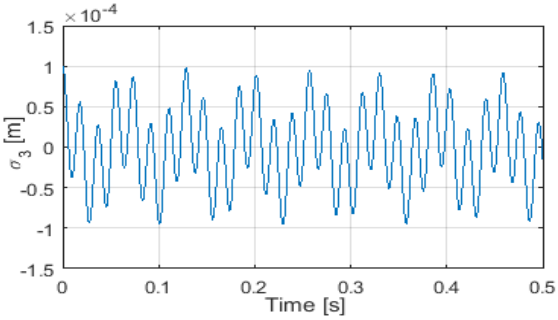

Fig. 8 Performance of the modal coordinate σ_3

The free vibration responses of flexible pectoral fin part are shown in the Fig. 6-8. The modal coordinates of fin have largely different amplitudes, the higher numerical order of mode, the lower the amplitude modal coordinate. Therefore, to reduce the time consumption in the simulation, we only carry on some of the first modes and accept a certain error.

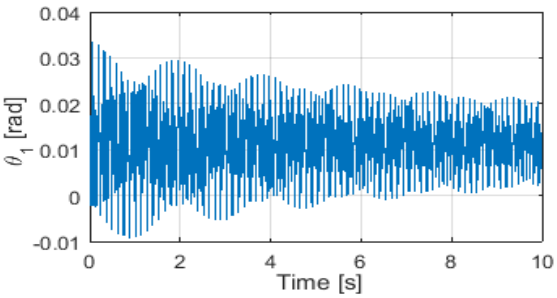

Fig. 9 Performance of the angle of link 2

The performance of guiding angle of flexible fin (link 2) vibrates in the small amplitude. This is too small to produce the large displacement of tip-fin shown in the Fig. 10.

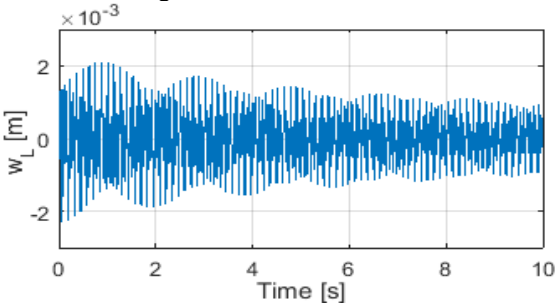

Fig. 10 The displacement of tip-flexible fin

B. Forced vibration mode

To verify the performance of system when the external torques are applied. The simulation is carried on with the input torques are bang-bang signal for the link 1 and the sinusoidal wave for link 2. The inputs are illustrated in the Fig. 11. The maximum and minimum values and the retention period of the bang-bang input are $\pm 0.0045[N]$ and $0.15[s]$ respectively. The sinusoidal wave input is given by below expression:

$\tau_1 = 0.001.\sin\left(3.\pi.t - 2\pi/3\right)$.

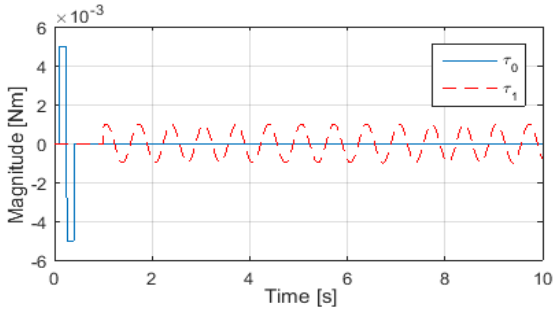

Fig. 11 Two input torques applied to link 1, 2

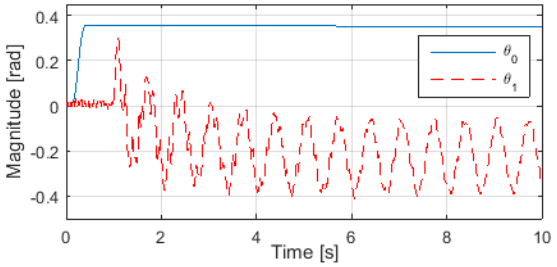

Fig. 12 Performance of the angles guiding pectoral fin

The responses of angles of link 1 and link 2 are shown in the Fig. 12. Due to uncontrolled angle position, the mean line of θ_1 doesn't converge to zero value and it depends on initial excited states. The phase response of θ_1 is approximately same as the phase of input torque. The displacement of tip-fin described in the Fig. 13 is inverse in the phase comparison with input torque. It is reasonable when the pectoral fin owns the appropriate softness in the range of excitation.

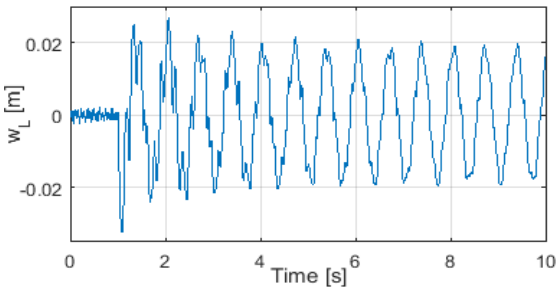

Fig. 13 The displacement of tip-fin

In the Fig. 13, we see that the deformation of tip-fin includes two parts, one is affected by the period of free vibration and another is when the external torque applied. The frequency of displacement generated by the external torque is equal the frequency of excitation.

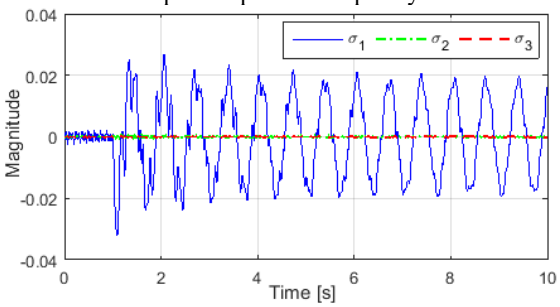

Fig. 14 The performance of modal coordinates

In the response of the modal coordinates, the first modal vibration is with the frequency about 1.5Hz when the external torque is supplied. Its amplitude is also very larger than the other mode. In general, it is the most important mode in non-resonant case.

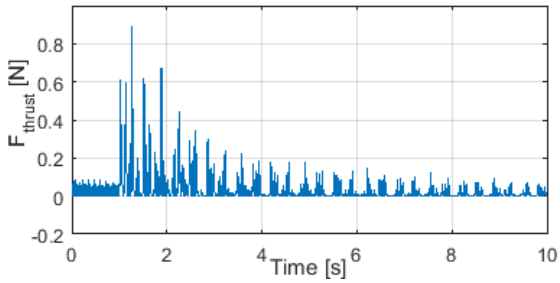

Fig. 15 The performance of the generated thrust

In the Fig. 15, the thrust force performance is discontinuous and its average value stabilizes over time. The thrust force generated by natural vibration of the flexible fin part is quite small. The simulation results show the important properties of the soft pectoral fin in oscillating mode in fluid environment. These aim to choose the frequency, amplitude of excitation torque relevantly.

5. Conclusion

The accuracy of modeling is very important for solving problems in robotic fish. E.g. in the controller design, the optimization of geometry fin of motion trajectory. The paper presents the approach of building the mathematical equation expressed the dynamic motion of the soft pectoral fin with 2-DOFs mechanism in the direction of simplicity and clarity. The established differential equations base on AMM and Lagrange' method. The fluid force impacts on along the surface of fin is model by the Morison's formula, in which, the added mass and damping effect is considered. Some simulation implemented to verify the feasibility of vibration performances. We are carrying out the experiments to evaluate the agreement of theory model and practical model. The modeling

with the full configuration of body and fins will be also implemented in the future.

7. References

[1] W. Yu, T. Rui, X. Guoliang, W. Jianxun, and T. Xiaobo. (2014). Profiling Aquatic Diffusion Process Using Robotic Sensor Networks, *IEEE Transactions on Mobile Computing,* vol. 13(4), 2014, pp. 880-893.

[2] C. M. Breder and N. Y. Z. Society. (1926). The Locomotion of Fishes, New York Zoological Society,

[3] J. Yu, Z. Su, M. Wang, M. Tan, and J. Zhang. (2012). Control of Yaw and Pitch Maneuvers of a Multilink Dolphin Robot, *IEEE Transactions on Robotics,* vol. 28(2), 2012, pp. 318-329.

[4] S. Zongshuai, Y. Junzhi, T. Min, and Z. Jianwei. (2014). Implementing Flexible and Fast Turning Maneuvers of a Multijoint Robotic Fish, *IEEE/ASME Transactions on Mechatronics,* vol. 19(1), 2014, pp. 329-338.

[5] T. Q. Vo, H. S. Kim, and B. R. Lee. (2009). Propulsive Velocity Optimization of 3-Joint Fish Robot Using Genetic-Hill Climbing Algorithm, *Journal of Bionic Engineering,* vol. 6(4), 2009, pp. 415-429.

[6] B. Sanaz Bazaz and T. Xiaobo. (2016). Bio-inspired flexible joints with passive feathering for robotic fish pectoral fins, *Bioinspiration & Biomimetics,* vol. 11(3), 2016, p. 036009.

[7] A. A. Farahani, A. A. Suratgar, and H. A. Talebi. (2014). Dynamics model and adaptive control of underwater fish-like micro mobile robot with PZT actuator, paper presented in *Robotics and Mechatronics (ICRoM), 2014 Second RSI/ISM International Conference on*.

[8] J. J. Hubbard, M. Fleming, V. Palmre, D. Pugal, K. J. Kim, and K. K. Leang. (2014). Monolithic IPMC Fins for Propulsion and Maneuvering in Bioinspired Underwater Robotics, *IEEE Journal of Oceanic Engineering,* vol. 39(3), 2014, pp. 540-551.

[9] Z. Shiwu, L. Bo, W. Lei, Y. Qin, L. Kin Huat, and Y. Jie. (2014). Design and Implementation of a Lightweight Bioinspired Pectoral Fin Driven by SMA, *IEEE/ASME Transactions on Mechatronics,* vol. 19(6), 2014, pp. 1773--1785.

[10] V. Kopman, J. Laut, F. Acquaviva, A. Rizzo, and M. Porfiri. (2015). Dynamic Modeling of a Robotic Fish Propelled by a Compliant Tail, *IEEE Journal of Oceanic Engineering,* vol. 40(1), 2015, pp. 209--221.

[11] V. Kopman and M. Porfiri. (2013). Design, Modeling, and Characterization of a Miniature Robotic Fish for Research and Education in Biomimetics and Bioinspiration, *IEEE/ASME Transactions on Mechatronics,* vol. 18(2), 2013, pp. 471-483.

[12] P. L. Nguyen, V. P. Do, and B. R. Lee. (2013). Dynamic Modeling and Experiment of a Fish Robot with a Flexible Tail Fin, *Journal of Bionic Engineering,* vol. 10(1), 2013, pp. 39-45.

[13] C. Tang and X.-y. Lu. (2016). Self-propulsion of a three-dimensional flapping flexible plate, *Journal of Hydrodynamics, Ser. B,* vol. 28(1), 2016, pp. 1-9.

[14] L. Wang, M. Xu, B. Liu, K. H. Low, J. Yang, and S. Zhang. (2013). A Three-Dimensional Kinematics Analysis of a Koi Carp Pectoral Fin by Digital Image Processing, *Journal of Bionic Engineering,* vol. 10(2), 2013, pp. 210-221.

[15] M. Sfakiotakis, D. M. Lane, and J. B. C. Davies. (1999). Review of fish swimming modes for aquatic locomotion, *IEEE Journal of Oceanic Engineering,* vol. 24(2), 1999, pp. 237--252.

[16] V. A. Pham, K. A. Hoang, T. T. Nguyen, and T. Q. Vo. (2016). A Study on Moving Direction and Surge Velocity Control of a Carangiform Fish Robot Driven by Flexible Pectoral Fins, in AETA 2015: Recent Advances in Electrical Engineering and Related Sciences, Springer International Publishing, Cham.

[17] R. Shuai, C. Yueri, B. Shusheng, Z. Lige, and Z. Houxiang. (2013). Kinematic analysis and design of a robotic fish using flapping and flexional pectoral fins for propulsion, paper presented in *IEEE International Conference on Robotics and Biomimetics (ROBIO)*.

[18] P. L. Nguyen, V. P. Do, and B. R. Lee. (2013). Dynamic Modeling of a Non-Uniform Flexible Tail for a Robotic Fish, *Journal of Bionic Engineering,* vol. 10(2), 2013, pp. 201-209.

[19] E. B. Magrab. (2012). Vibrations of Elastic Systems, Springer

[20] M. J. Lighthill. (1971). Large-Amplitude Elongated-Body Theory of Fish Locomotion, *Proceedings of the Royal Society of London. Series B, Biological Sciences,* vol. 179(1055), 1971, pp. 125--138.